NMR Solution Structure of Viscotoxin C1 from Viscum Album Species Coloratum ohwi: Toward a Structure−Function Analysis of Viscotoxins

ARTICLE *in* BIOCHEMISTRY · DECEMBER 2003

Impact Factor: 3.02 · DOI: 10.1021/bi034762t · Source: PubMed

9 AUTHORS, INCLUDING:

Federico Fogolari
University of Udine
127 PUBLICATIONS **2,942** CITATIONS

SEE PROFILE

Laura Ragona
Italian National Research Council
75 PUBLICATIONS **1,476** CITATIONS

SEE PROFILE

Henriette Molinari
Italian National Research Council
143 PUBLICATIONS **3,272** CITATIONS

SEE PROFILE

NMR Solution Structure of Viscotoxin C1 from Viscum Album Species *Coloratum ohwi*: Toward a Structure−Function Analysis of Viscotoxins†

Silvia Romagnoli,‡ Federico Fogolari,‡ Maddalena Catalano,§ Lucia Zetta,§ Gerhard Schaller,|| Konrad Urech,|| Matteo Giannattasio,⊥ Laura Ragona,§ and Henriette Molinari*,‡

Dipartimento Scientifico e Tecnologico, Università degli Studi di Verona, Strada le Grazie 15, 37134 Verona, Italy, Laboratorio NMR, ISMAC-CNR, Via Bassini 15, 20133 Milano, Italy, Verein fur Krebsforschung, Hiscia Institute, 4144 Arlesheim, Switzerland, and Dipartimento di Arboricoltura, Botanica e Patologia Vegetale, Facoltà di Agraria, Università di Napoli, Portici, 80100 Napoli, Italy

Received May 9, 2003; Revised Manuscript Received September 5, 2003

ABSTRACT: The high resolution three-dimensional structure of the newly discovered plant viscotoxin C1, from the Asiatic *Viscum album* ssp. *Coloratum ohwi*, has been determined in solution by ^{1}H NMR spectroscopy at pH 3.6 and 285 K. The viscotoxin C1-fold, consisting of a helix−turn−helix motif and a short stretch of an antiparralel β-sheet is very similar to that found for the highly similar viscotoxins A2 and A3 and for other related thionins. Different functional properties of members of the thionin family are discussed here in light of the structural and electrostatic properties. Among the very homologous family of α- and β-thionins, known for their antimicrobial activity, the viscotoxin subfamily differs from the other members because of its high toxicity against tumoral cells. Key residues for the modulation of viscotoxin cytotoxicity have been identified on the basis of sequence and structural alignment.

Viscotoxins are a group of basic low molecular weight proteins (MW approximately 5000 Da) found in the European mistletoe subspecies of *Viscum album*. On the basis of sequence homology, they have been classified as belonging to the α- and β-thionin family (*1*, *2*). Thionins include several plant proteins from cereals (hordothionins, purothionins, and avenothionins), *Brassicaceae* (crambins), and *Pyrularia pubera* and *Viscaceae* (viscotoxins from European mistletoes and phoratoxins from American mistletoes *Phoradendron* sp.). The main characteristic of all thionins, except crambin, is their toxic effect on different biological systems: evidences of bactericidal and fungicidal properties as well as toxicity in insects were reported (*3*, *4*). Thionin toxicity is exerted through cell membrane destabilization and disruption, but the mechanism of action is not yet fully understood. To account for this generalized toxicity, it was proposed that thionins induce ion channel formation in cell membranes, causing the dissipation of ion concentration gradients (*5*). An alternative theory suggests that thionins lead to cell membrane breakdown through purely electrostatic interactions with the negatively charged phospholipids (*6*).

Viscotoxins share a high sequence similarity with thionins (*7*), and their cysteine residues, all involved in disulfide bridges, are kept in conserved positions within the amino acid sequence defining a structural motif, known as a concentric motif. This kind of disulfide pattern is suggested to be able to stabilize a common structure occurring in various small proteins able to interact with cell membranes (*1*). Besides the poisonous effects on the whole organism, viscotoxins have been reported to be cytotoxic against many tumoral cell lines including *Yoshida sarcoma* cells (*8*, *9*), K 562 human myelogenous leukaemia (*9*), and HeLa cells (*10*).

Until now, several viscotoxin isoforms have been characterized; namely, viscotoxins A1, A2, A3, B, and 1-PS. These proteins are highly basic, possessing three to four arginines and three to four lysines. Their alignment together with related α- and β-thionins is reported in Figure 1. For viscotoxin A3, displaying the highest toxicity against *Y. sarcoma* cells, the three-dimensional structure has been previously reported by our group (*7*), and viscotoxin A2 has been recently deposited (PDB 1JMN) (*11*). Here, we report the discovery and the NMR[1] structural and electrostatic characterization of a new isoform, viscotoxin C1, from the Asiatic *V. album* ssp. *C. ohwi*. Structure and electrostatic properties of the other isoforms A1, B, and 1-PS were obtained on the basis of homology modeling and discussed as a function of the measured cytotoxicity against *Y. sarcoma* cell lines.

MATERIALS AND METHODS

Sample Preparation. Viscotoxin C1 was detected by bioactivity guided fractionation of acetic acid (0.2 M) extracts from leaves of *V. album* ssp. *C. ohwi* using the viscotoxin

† S.R. acknowledges CNR for Fellowship 201.22/04.

* To whom correspondence should be addressed. Tel.: +39 45 8027097. Fax: +39 45 8027929. E-mail: molinari@sci.univr.it.

‡ Università degli Studi di Verona.

§ ISMAC-CNR.

|| Hiscia Institute.

⊥ Università di Napoli.

[1] Abbreviations: NMR, nuclear magnetic resonance; NOE, nuclear Overhauser enhancement; DQF−COSY, double quantum filtered−correlation spectroscopy; TOCSY, total correlation spectroscopy; NOESY, nuclear Overhauser enhancement spectroscopy; HPLC, high performance liquid chromatography; SDS−PAGE, sodium dodecyl sulfate−polyacrylamide gel electrophoresis; RMSD, root mean square deviation.

10.1021/bi034762t CCC: $25.00
Published on Web 10/10/2003

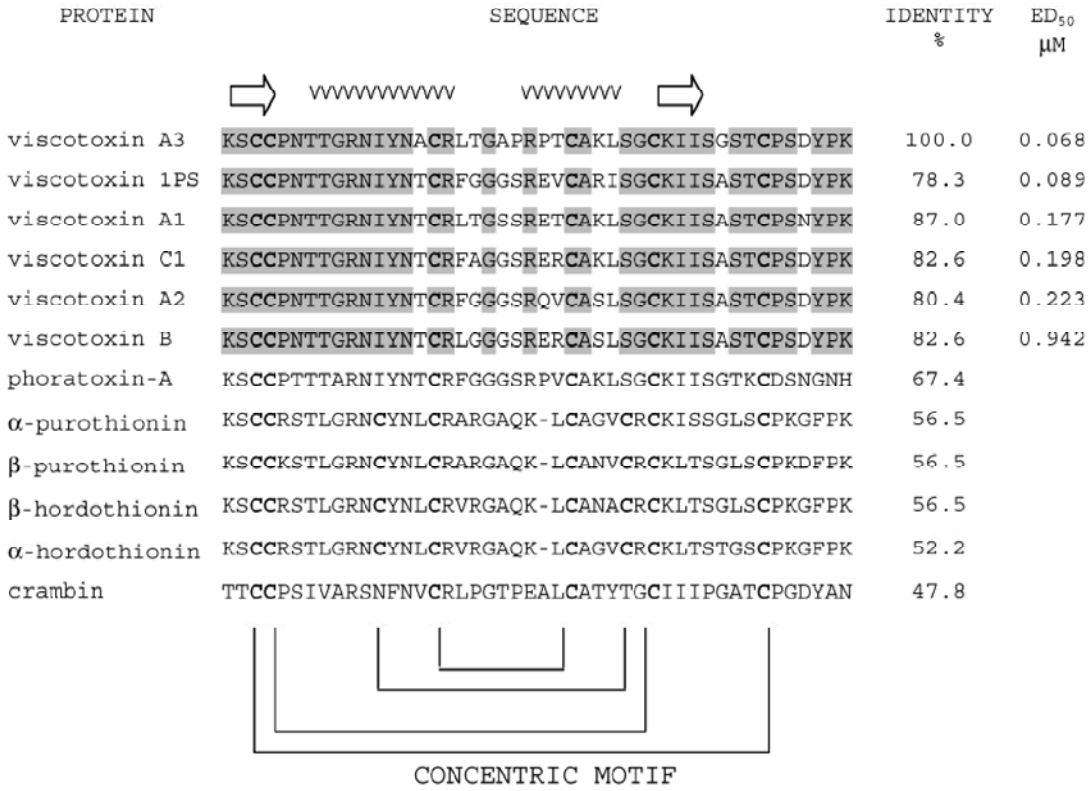

FIGURE 1: Alignment of all reported viscotoxin isoforms, listed in order of decreasing cytotoxicity (ED_{50}) together with related α- and β-thionins of known structure. Conserved residues in the viscotoxin sequences are shaded. Sequence identity and biological activity data (ED_{50}) are reported in the last two columns. Secondary structural elements of viscotoxin A3 are indicated. The disulfide bridge pattern, known as a concentric motif, is shown.

sensitive *Y. sarcoma* cells (*9*). The purification procedure was the same as described for viscotoxin A3 and B (*8*). Samples for NMR studies were 1 mM in 50 mM H_3PO_4/NaOH buffer at pH = 3.6.

Viscotoxin C1 Primary Structure Characterization. Viscotoxin C1 primary structure was determined by Edman degradation coupled to HPLC, NMR proton assignment, and mass spectrometry. A molecular weight of 4945.5 Da over an expected value of 4946.6 was measured.

NMR Spectroscopy. NMR spectra were acquired on a Bruker DRX spectrometer operating at 500.13 MHz. Standard homonuclear ^{1}H DQF−COSY (*12*), TOCSY (*13*), and NOESY (*14*) experiments were recorded, employing mixing times in the range of 20−100 ms for TOCSY and 60−150 ms for NOESY. Data matrixes of 4096 × 512 points were acquired in f_2 and f_1, respectively, and 120 scans were accumulated with a sweep width of 5838 Hz in both dimensions. Water suppression was achieved with gradients by a 3-9-19 pulse sequence (*14*) or using excitation sculpting (*15*). All NMR experiments were performed at variable temperatures in the range of 280−295 K. Spectra were processed using XWINNMR. Analysis of spectra and cross-peak volumes was performed using XEASY software (*16*). All chemical shifts were referenced to the methyl resonance of 3-(trimethylsilyl)-propionic acid-d_4 sodium salt (TSP) dissolved in the same buffer solution. Secondary chemical shift maps were obtained using as a reference the random coil chemical shifts reported by Wishart et al. (*17*). Assignment of spin systems to individual amino acids was achieved by using DQF−COSY and TOCSY spectra acquired at 285 K, while complete resonance assignment was obtained by the combined use of TOCSY and NOESY spectra, following the sequential assignment strategy (*18*). The obtained assignments were extended at 295 K, and NOESY experiments with different mixing times (60, 100, and 150 ms) and DQF−COSY were performed at all the selected temperatures to check for ambiguous assignments. A single H/D exchange experiment was performed after exchanging the protein in deuterated buffer. Since the protein concentration was quite low (<0.7 mM), acquisition times of 72 h were employed for TOCSY and NOESY experiments. Amide protons stable for at least one week gave us some indication of their involvement in H-bonds.

Structure Calculations. Calculated structures were obtained from restrained simulations using DYANA (*19*) followed by energy minimization using the AMBER force field, as implemented by the program DISCOVER (Molecular Simulations, San Diego, CA). The calibration of the NOESY peak volume was performed on the NOESY spectrum acquired in aqueous solution at T = 285 K, with a mixing time of 100 ms, on the basis of the $H^{\gamma 3}-H^{\delta 2}$ distance of P_{41}, corresponding to an internuclear separation of 3.04 Å. Calibration was executed using the tools of the DYANA package (*20*), and the obtained list of distance restraints was used as input for DYANA calculations. In all the cases where severe overlap prevented us from quantifying cross-peak volumes, a distance of 4 Å was assumed between the interacting protons. A total of 845 interproton distances were used as input for structure calculation; standard procedures were used to remove irrelevant restraints, thus obtaining 631 final restraints composed of 224 intraresidue, 159 short range, 125 medium range, and 123 long range distances. The NOE

restraints were supplemented by three types of restraints: (i) 24 distance restraints for 12 backbone hydrogen bonds. Hydrogen bond formation or solvent exclusion was assumed to account for the slow exchanging amide protons; for each hydrogen bond, the N−O and NH−O distances were assigned an upper limit value of 3.00 and 2.00 Å, respectively. The partners for all hydrogen bonds were assigned on the basis of preliminary structures obtained by imposing only NOE restraints; (ii) 18 distance restraints for the three disulfide bonds; for each disulfide bridge an upper and lower limit value was imposed to the three distance restraints that define an S−S bond: S_i−S_j (2.00−2.10 Å) S_i−$C_{\beta j}$ (3.00−3.10 Å), and S_j−$C_{\beta i}$ (3.00−3.10 Å); and (iii) 18 ϕ backbone torsion angle restraints derived from $^3J_{HN\alpha}$ coupling constants whose values were estimated by the separation of extrema in the dispersive and absorptive peaks of DQF−COSY spectra (*12*). ϕ angle restraints of $-133 \pm 30°$ for $^3J_{HN\alpha}$ coupling constants greater than 8.0 Hz and $-55 \pm 30°$ for $^3J_{HN\alpha}$ coupling constants smaller than 4.0 Hz were used for calculations. Two-hundred calculations were initially performed with the program DYANA, and the 20 resulting conformers with the lowest residual target function values (resulting from van der Waals and restraint violations) were analyzed. The restraints were reexamined in view of consistent violations and relaxed where necessary. This procedure was repeated until no consistent violations were found in half or more of the structures. After this step, 600 new calculations were started; the 20 structures selected on the basis of the lowest target function (ranging from 0.34 to 0.52) showed no violations larger than 0.20 Å and were then subjected to energy minimization using the AMBER force field with a distance dependent dielectric constant ($\epsilon = 4.0$) as implemented in the program Discover (Molecular Simulations, San Diego, CA). The 10 structures with the lowest potential energy were then selected for further analysis. INSIGHT II (Molecular Simulations, San Diego, CA) and Swiss-Pdb Viewer (*21*) programs were used to visually inspect the structures.

Modeling. Until now, six viscotoxin isoforms from European mistletoe have been isolated and sequenced, but a structural characterization was previously reported only for viscotoxin A3 (*7*) and A2 (*11*). A1, B, and 1-PS three-dimensional structures (showing at least 78.3% identity and 93.5% similarity with isoform A3) were obtained by homology modeling using the software Geno3D (*22*), employing viscotoxin A3 as template structure (PDB 1ED0).

Electrostatic Potential Map Calculations. Electrostatic potential maps for C1, A1, A2, A3, B, and 1-PS viscotoxins were computed using a Poisson−Boltzmann based methodology (*23*) as implemented in the software package UHBD (*24*). Partial atomic charges and van der Waals radii were taken from the CHARMM force field (*25*). Molecular and solvent dielectric constants were set to 4.0 and 80.0, respectively, the ionic strength was set to 100 mM, and the probe radius for generating the dielectric map was set to 1.4 Å. A standard procedure was employed, solving first the Poisson−Boltzmann equation on a coarse grid of 60 × 60 × 60 points with 2.5 Å spacing imposing the sum of the atomic Debye−Hückel potential as the boundary condition and then focusing on the molecule using a finer grid of 65 × 65 × 65 points with a spacing of 0.8 Å. The GRASP program (*26*) was used to visualize the electrostatic potential surfaces.

Cytotoxicity Assay. Cytotoxicity of purified viscotoxin C1 was detected by measuring the inhibition of ^{3}H-thymidine incorporation into *Y. Sarcoma* cells as previously described for viscotoxin A1, A2, A3, B, and 1-PS (*8*). Each assay was done at least in triplicate. The concentration of substance inhibiting 50% of ^{3}H-thymidine corresponds to the ED_{50} and was defined as 1 inhibitory unit.

RESULTS

Primary Structure Determination. The sequence of viscotoxin C1, as obtained by Edman degradation coupled to HPLC, showed few ambiguities relative to four residues: residue 38 was identified with the same probability as an alanine or serine, and the last three residues were only supposed to be Y_{44}, P_{45}, and K_{46} due to a low signal. The sequence, completely determined through the NMR sequential assignment and confirmed by mass spectrometry, is the following: KSCCPNTTGR$_{10}$NIYNTCRFAG$_{20}$GSRERCA-KLS$_{30}$GCKIISASTC$_{40}$PSDYPK (Swiss-Prot accession number P83554).

Assignment of Spin Systems. Complete proton assignment of viscotoxin C1 was achieved following the sequential resonance assignment procedure (*18*) by the combined use of two-dimensional ^{1}H DQF−COSY, TOCSY, and NOESY experiments. The list of proton chemical shifts, as obtained from spectra acquired at pH = 3.6 and 285 K, is reported in Table 1. Figure 2 shows a portion of a TOCSY spectrum, illustrating through-bond connectivities between the amide and the aliphatic protons.

Structure Calculations. A summary of NOE connectivities is reported in Figure 3. The presence of H-bonds was exploited for structure calculations. The partners for all hydrogen bonds were assigned on the basis of preliminary structure calculations, as obtained by imposing only NOE restraints in the procedure of DYANA molecular dynamics, as described in the Materials and Methods.

Two α-helices, helix I (7−19) and helix II (23−30), have been identified on the basis of short d_{NN} (i, $i+1$), $d_{\alpha N}$ (i, $i+3$), and $d_{\alpha\beta}$ (i, $i+3$) distances and by slow exchanging amide protons (Figure 3). The two short antiparallel β-strands (*1*−*3*, *33*−*35*) were identified on the basis of typical H^{α}_i−H^{α}_j NOEs between residues S_2 and I_{34} and C_4 and C_{32}; by H^{α}_i−H^{N}_j NOEs between S_2 and I_{35}, C_4 and K_{33}, and I_{34} and C_3; and by $H^{\alpha}C_{32}$ and $H^{\delta}P_5$.

The analysis of the spectra acquired at 285 K in ^2H_2O led to the identification of a few long range interactions ($H^{\delta}P_5$−$H^{\epsilon}Y_{44}$, $H^{\delta}P_5$−$H^{\delta}Y_{44}$, $H^{\alpha}C_{32}$−$H^{\delta}Y_{44}$, and $H^{\alpha}C_{32}$−$H^{\epsilon}Y_{44}$). These NOEs suggest that the C-terminal end of the molecule is anchored to the rest of the structure, in agreement with the presence of the C_4−C_{32} disulfide bridge.

The superposition of the 10 final structures of viscotoxin C1 (PDB 1ORL) is shown in Figure 4. For a survey of the conformational restraints and the quality of the structure determination, see Table 2. The average RMSD values in the region of 2−45 are 0.57 ± 0.16 and 1.22 ± 0.17 Å for the backbone and all heavy atoms, respectively (Table 2). The C1 structure resembles a capital letter L, in which the long arm of the L is formed by the two α-helices running in opposite directions and connected by a short turn (residues

Table 1: Proton Resonance Assignments (δ, ppm) for Viscotoxin C1 at 285 K and pH 3.6

residue	HN	H^{α}	H^{β}	H^{γ}	H^{δ}	others
Lys^{1}		4.18	1.83−1.94	1.31−1.40	1.52−1.58	H^{ϵ} = 3.07 H^{ξ} = 7.56
Ser^{2}	8.91	4.98	2.84−3.77			
Cys^{3}	9.09	5.01	2.24−4.42			
Cys^{4}	9.42	5.27	2.67−2.70			
Pro^{5}		4.42	2.02−2.07	2.26	3.81−3.99	
Asn^{6}	6.94	4.55	3.30		6.99−7.87	
Thr^{7}	9.03	3.89	4.17	1.30		
Thr^{8}	8.20	3.98	4.09	1.29		
Gly^{9}	8.67	3.59−4.05				
Arg^{10}	7.68	4.58	2.14	1.70 1.93	3.30 3.48	H^{ϵ} = 8.81
Asn^{11}	8.46	4.61	2.97−3.06		6.95−7.69	
Ile^{12}	8.51	3.69	1.86	CH_2 = 1.11−1.95 CH_3 = 0.86	0.92	
Tyr^{13}	8.98	3.67	3.13			$H^{2,6}$ = 6.89 $H^{3,5}$ = 6.83
Asn^{14}	9.01	4.19	2.74−3.08		6.98−7.80	
Thr^{15}	8.36	3.95	4.25	1.28		
Cys^{16}	8.04	4.20	3.02−3.29			
Arg^{17}	8.57	4.01	1.63−1.79	0.89−1.18	2.47−3.03	H^{ϵ} = 7.23 H^{ξ} = 6.60−7.04
Phe^{18}	8.72	4.39	3.26			$H^{2,6}$ = 7.29 $H^{3,5}$ = 7.34
Ala^{19}	7.42	4.38	1.57			
Gly^{20}	7.80	3.70−4.37				
Gly^{21}	8.25	3.44−4.11				
Ser^{22}	8.57	4.35	4.17−4.41			
Arg^{23}	9.11	3.83	1.72−1.76	1.62−1.87	3.05−3.26	H^{ϵ} = 7.74
Glu^{24}	8.69	3.98	1.95−2.07	2.35−2.45		
Arg^{25}	8.04	4.03	1.83−1.88	1.47−1.64	3.14−3.26	H^{ϵ} = 7.39
Cys^{26}	8.75	4.65	2.36−2.71			
Ala^{27}	9.38	3.95	1.52			
Lys^{28}	7.53	4.10	2.03−2.05	1.50−1.59	1.72	H^{ϵ} = 3.00
Leu^{29}	7.91	4.19	1.70−1.73	1.68	0.88−0.92	
Ser^{30}	7.65	4.30	3.76−4.74	5.85		
Gly^{31}	8.03	4.39−3.95				
Cys^{32}	8.04	4.96	2.38−2.98			
Lys^{33}	9.00	4.50	1.05	0.70−1.28	0.94−1.10	H^{ϵ} = 2.42−2.49
Ile^{34}	8.51	4.55	1.94	CH_2 = 1.09−1.33 CH_3 = 0.72	0.62	
Ile^{35}	8.81	4.68	1.95	CH_2 = 1.00−1.32 CH_3 = 0.77	0.71	
Ser^{36}	8.77	4.60	3.87			
Ala^{37}	7.24	4.51	1.53			
Ser^{38}	8.44	4.37	3.93−3.96			
Thr^{39}	7.25	4.45	3.94	1.16		
Cys^{40}	8.93	4.77	2.57−3.80			
Pro^{41}		4.66	2.35−2.39	2.02−2.19	3.66−3.80	
Ser^{42}	8.81	4.02	3.91			
Asp^{43}	8.74	4.47	2.67			
Tyr^{44}	7.66	4.36	2.36−2.45			$H^{2,6}$ = 6.76 $H^{3,5}$ = 6.88
Pro^{45}		4.46	2.00	1.62−2.02	3.35	
Lys^{46}	8.31	4.34	1.15	1.77	1.47−1.60	H^{ϵ} = 2.91−2.98 H^{ξ} = 7.61

20−22), while the short arm is formed by the antiparallel β-sheet together with the C-terminal region. The overall topology of viscotoxin C1 is very similar to viscotoxin A3 (*7*) (RMSD $_{bb\ 2-45}$ = 1.20 Å) and A2 (*11*) (RMSD $_{bb\ 2-45}$ = 1.38 Å) and to those of other thionins previously reported (*27*−*30*).

Electrostatic Properties. Electrostatic potential maps for viscotoxins A3, C1, A1, A2, B, and 1-PS have been computed. Viscotoxins A3, A1, and C1 bear a 6.0 unit net charge, viscotoxins B and 1-PS bear a 5.0 unit net charge, and the A2 isoform bears a 4 unit net charge. The six viscotoxins share a common pattern of electrostatic potential at the surface: a net positive potential is differently distributed on the proteins surface, defining two molecular faces. One face of the molecule is characterized by a high positive electrostatic potential that corresponds to the surface enclosed by the two α-helices, while the other face displays a less extended positive electrostatic potential. The electrostatic potential at the surface is shown only for the A3 and C1 isoform (Figure 5) since the other structures show a similar pattern of charge.

Cytotoxicity Assay. To correlate structural and electrostatic properties of the different viscotoxin isoforms with their biological activity against tumors, their cytotoxicity was analyzed by measuring the inhibition of ^{3}H-thymidine incorporation into *Y. sarcoma* cells, as previously described (*8*, *9*). The toxicity values obtained were the following: viscotoxin A3, ED_{50} = 0.068 μM; 1-PS, ED_{50} = 0.089 μM;

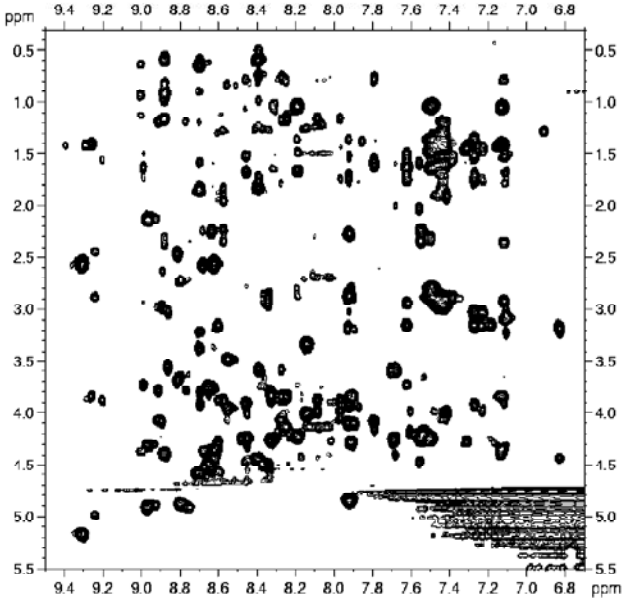

FIGURE 2: Fingerprint region of 500 MHz ^{1}H TOCSY spectrum (isotropic mixing 50 ms) of viscotoxin C1 (1 mM) in aqueous 50 mM H_3PO_4/NaOH buffer ($^1H_2O/^2H_2O$, 90:10, v/v), pH 3.6, 285 K.

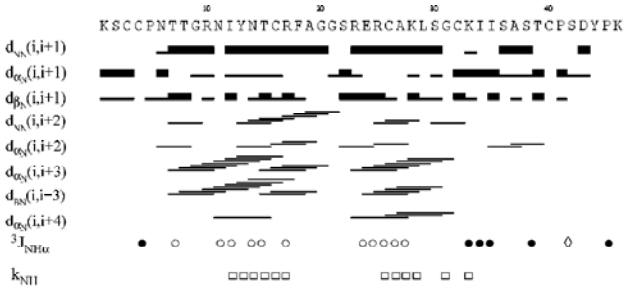

FIGURE 3: Summary of NMR data used to deduce viscotoxin C1 secondary structure. The notation $d_{NN,\ \alpha N,\ \beta N,\ \alpha\beta}$ (i, j) indicates the NOE intensity observed for the protons H^N, H^α, and H^β of residue i with H^N and H^β of residue j; the thickness of the bar indicates the relative normalized intensity of the NOE. The $^3J_{HN\alpha}$ are three-bond coupling constants between H^N and H^α, where the symbols represent the following: ○ helical values < 4.0 Hz, ● β-sheet-like values > 8 Hz, and ◇ values in the range of 4−8 Hz. Exchange rates, k_{NH}, are reported in the last line to identify residues with sufficiently slow amide exchange rates to enable observation of the H^N-H^α cross-peaks in a TOCSY spectrum recorded 144 h after exchanging the buffer against a deuterated solution at pH = 3.6.

A1, ED_{50} = 0.177 μM; C1, ED_{50} = 0.198 μM; A2, ED_{50} = 0.223 μM; and B, ED_{50} = 0.942 μM (Figure 1). The data show that the newly identified C1 isoform displays an intermediate toxicity with respect to the most toxic A3 and 1PS isoforms.

DISCUSSION

The structural comparison of viscotoxins C1, A3, and A2 allows for the identification of a conserved hydrophobic cluster involving residues 12 and 13 (helix I), 27 and 29 (helix II), and 34 (C-terminal β-strand). These residues are conserved in all viscotoxin sequences, thus suggesting that this hydrophobic cluster bears some relevance for viscotoxin topology, stabilizing the packing of the two helices and of the β-sheet. The relevant role of this cluster is further underlined by its conservation in the other thionins of known structure.

Table 2: Conformational Restraints and Structural Parameters Determined Using DYANA

Restraints	
upper distance restraints	631
hydrogen bond restraints	24
torsion angle (ϕ) restraints	18
DYANA (20 Best Structures)	
target function (Å^2)	0.45 ± 0.05
average number of upper restraints violations >0.2 Å/structure	0.0
maximum violation (Å)	0.2
average number of angle restraints violations >5°/structure	0.0
⟨RMSD⟩ (2−45, backbone atoms)	0.7 ± 0.2
⟨RMSD⟩ (2−45, heavy atoms)	1.3 ± 0.2
Discover (AMBER Force Field) (10 Best Structures)	
total energy (kcal/mol)	−202 ± 6
bond energy (kcal/mol)	5.7 ± 0.2
angle energy (kcal/mol)	38 ± 1
torsion energy (kcal/mol)	49 ± 2
out of plane energy (kcal/mol)	0.9 ± 0.1
hydrogen bond energy (kcal/mol)	23 ± 1
lennard−Jones energy (kcal/mol)	−157 ± 2
Coulomb energy (kcal/mol)	−115 ± 3
restraining potential energy (kcal/mol)	8 ± 1
average number of upper restraints violations > 0.2 Å/structure	5 ± 3
maximum violation (Å)	0.4
average number of angle restraints violations > 5°/structure	0
maximum violation (degree)	0
⟨RMSD⟩ (2−45, backbone atoms) (Å)	0.57 ± 0.16
⟨RMSD⟩ (2−45, heavy atoms) (Å)	1.22 ± 0.17

It is worth mentioning that the two helices in viscotoxins are not amphipathic, and like other peptides with this same characteristic (such as, e.g., magainin1), display no haemolytic activity (*31*). It has been shown that while the N-terminal amphipathic helical structure is not required for the cytolytic activity toward negatively charged membranes and bacterial cells, it appears to be crucial for binding and insertion into zwitterionic membranes and for haemolytic activity (*32*). Haemolytic activity is clearly not a desirable feature in therapeutic peptides.

The presence of extended high positive potential areas at the molecule surface of all the studied viscotoxins hints at possible interaction sites with molecules bearing negative surface potential, such as the heads of cell membrane phospholipids. Indeed crambin, the only nontoxic thionin, bears a net unit charge equal to zero. The high isoelectric point of viscotoxins (pI > 9.0) ensures that the proteins remain charged at neutral pH and therefore will interact more strongly with negatively charged membrane phospholipids, such as phosphatidylserine membranes, rather than zwitterionic or neutral membranes.

We have previously suggested, from the comparison of the electrostatic properties of highly active viscotoxin A3 and the inactive crambin, that the loss of a positively charged residue at position 23 in crambin, together with the lack of other positively charged residues in the C-terminal region (namely, lysines 28, 33, and 46), are responsible for the absence of antimicrobial activity (*7*). A possible role in modulating viscotoxin biological activity may be played by residue 28, which is the only one among the four charged side chains exhibiting charge mutation in the different viscotoxin isoforms. However, even if the electrostatic

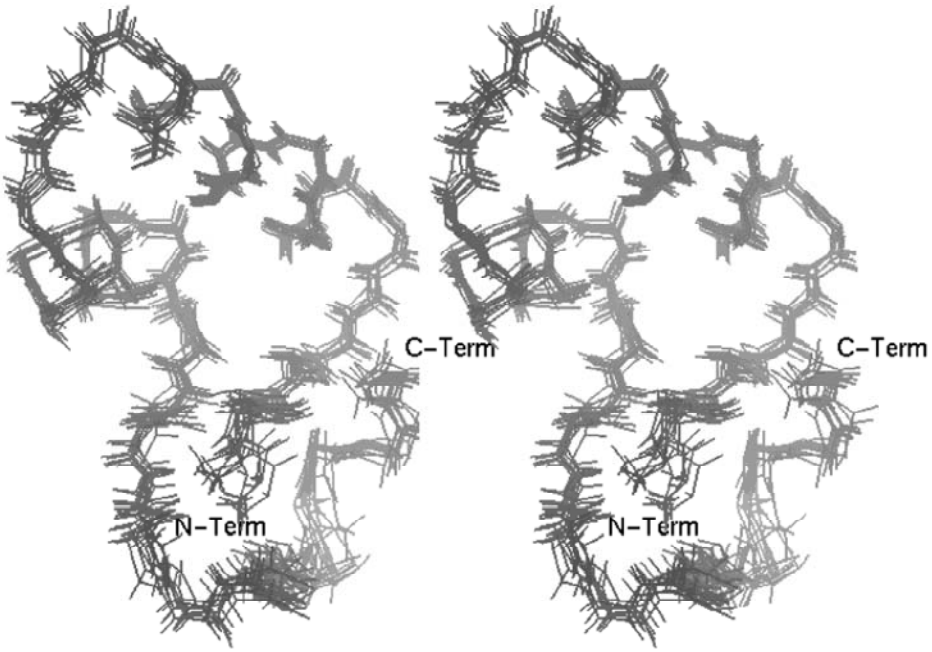

FIGURE 4: Superposition (stereoview) of the 10 final structures of viscotoxin C1 (PDB code: 1ORL), $RMSD_{bb\ 2-45} = 0.57 \pm 0.16$ Å.

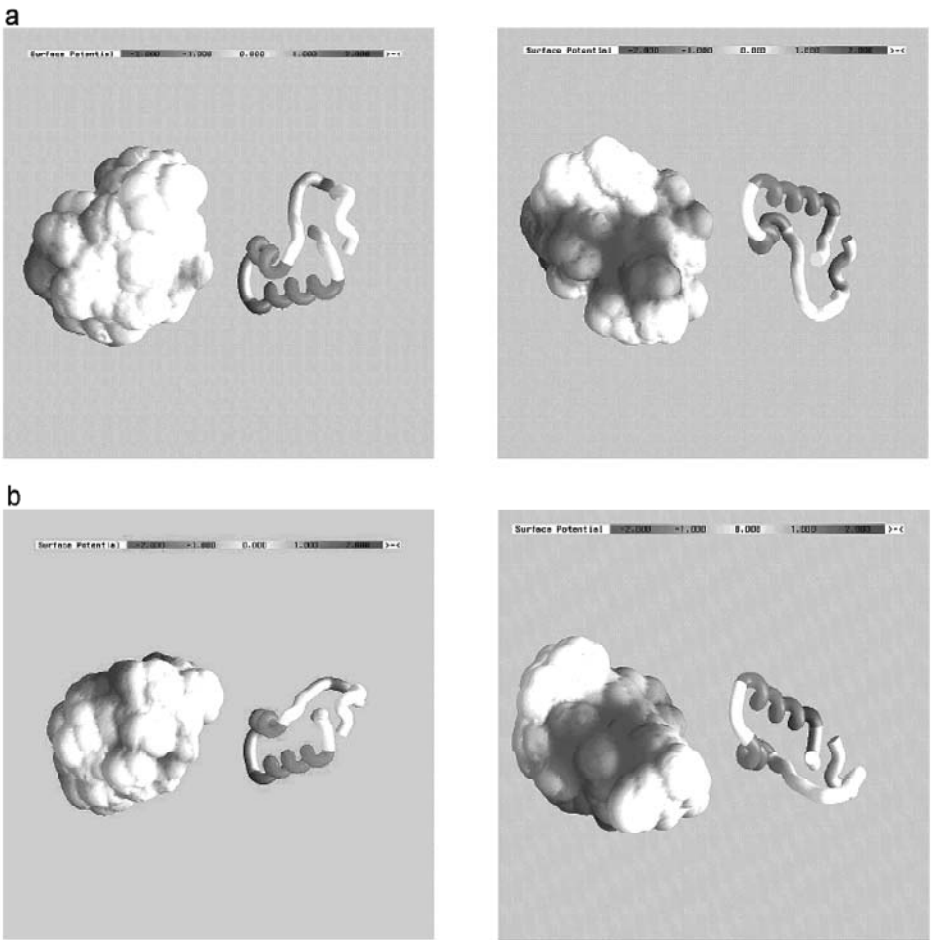

FIGURE 5: Electrostatic potential maps calculated for viscotoxins C1 (a) and A3 (b). Two views of the molecule are represented in the left and right panels.

surface properties of viscotoxins may provide structural evidence for an electrostatically driven interaction with negatively charged molecular targets, they are not sufficient to be assessed for the different levels of toxicity displayed, and a possible explanation should be searched in single residue mutations. Comparison of viscotoxin sequences (Figure 1) reveals that only 11 positions exhibit mutations (positions 15, 18, 19, 21, 22, 24, 25, 28, 29, 37, and 43),

mostly localized in the region of 15−29, including the C-terminal end of the first α-helix, the second α-helix, and the connecting loop. No mutation ever occurs in the regions involved in the formation of the short β-strands (*1*−*3*, *33*−*35*). Residues at positions 18, 29, and 43, exhibiting conservative mutations, were not considered relevant for the modulation of cytotoxicity. In view of the similar toxicity (ED_{50} in Figure 1) exhibited by the A3 and 1PS isoforms, residues 15, 22, and 37 (mutated only in viscotoxin A3) should not play a key role for the activity. The analysis of the role of specific mutations will therefore include only residues 19, 21, 24, 25, and 28. Interestingly, when pairs of sequences exhibiting the lowest number of mutations (three) are considered (i.e., the pairs C1/B, 1PS/A2, and A2/B), the relative role of every mutation can be discussed. Only one nonconservative mutation (K28S) is observed for the pair C1/B (ED_{50}C1 ∼ 5 ED_{50}B), underlying the relevance of a positively charged residue at position 28. Two nonconservative mutations (E24Q, R28S) are observed for the pair 1PS/A2, where only a 2.5-fold decrease in activity is measured, suggesting that the lack of a negatively charged residue at position 24 may enhance the toxicity. The 4-fold decrease in activity on going from the A2 to the B isoform can be ascribed to the two nonconservative mutations Q24E and V25R, where a further decrease in activity is possibly introduced by a positively charged residue at position 25. When the comparison is extended to the pair 1PS/B, where a 10-fold decrease in activity was measured, only two (V25R and R28S) out of the observed four mutations (F18L, V25R, R28S, and I29L) are nonconservative, strengthening our observation on the relevance of a noncharged residue at position 25 and of a positively charged residue at position 28. It is more difficult to account for the similar activity displayed by the A1/C1 pair where four out of five mutations are nonconservative. It would be, however, interesting to determine the A1 structure to clarify the relevance of the type and orientation of the side chain at position 25.

In a recent study, NMR and Fourier transform infrared spectroscopy have been used to show that β-purothionins, structurally similar to viscotoxins, strongly modify the lipid packing at the surface of the bilayer through electrostatic interactions between the cationic protein and the anionic phospholipid (*33*). Indeed, when the alignment analysis of viscotoxin isoforms is extended to related α- and β-thionins (Figure 1), charged residues are always located at positions 1, 10, 17, 23, 33, and 46, with the only exception being the inactive crambin. Although few studies have compared the in vitro activity of viscotoxins with that of other thionins, viscotoxins are known to be more toxic to eukariotic cells (*34*). For example, ED_{50} values measured on human tumor HeLa cells were in the range of 0.2−1.7 μg mL^{-1} for viscotoxins and 17 μg mL^{-1} for *Pyrularia* thionin. The higher viscotoxin toxicity nicely correlates with the presence of a charged residue at position 28, as discussed before.

The discussed key residues 19, 21, 24, 25, and 28 are highlighted on the superimposed C1, A3, and A2 viscotoxin structures (Figure 6a). It is clear from the figure that the most relevant residues 24, 25, and 28 are localized on the solvent exposed face of the second helix, which could behave as a recognition site for membrane interaction. In the three proteins, basic amino acids lie on one side of a plane roughly defined by the two helices (Figure 6b). The only exception

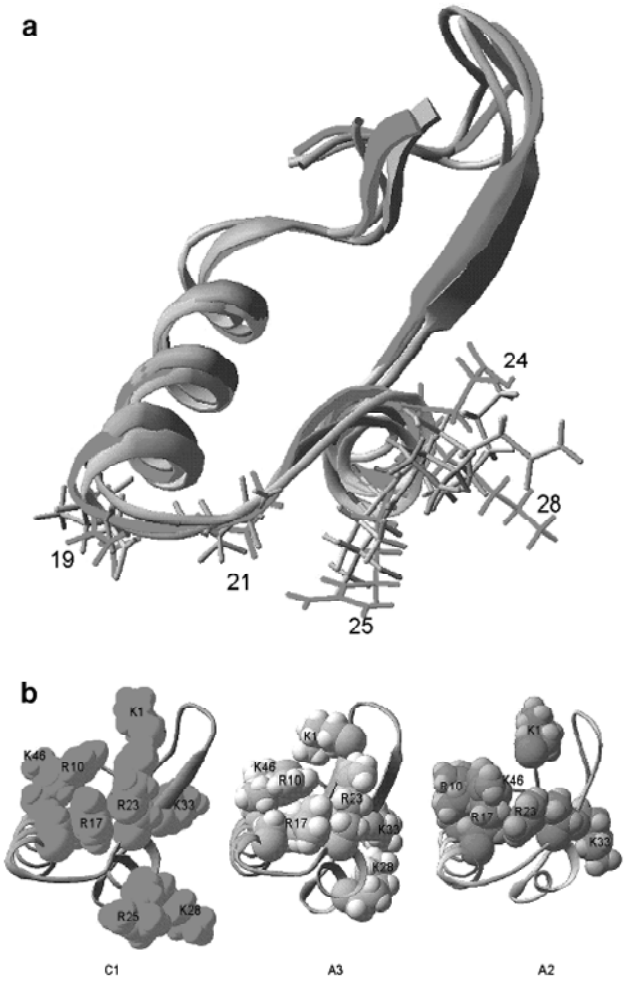

FIGURE 6: Comparison of C1 (green), A3 (dark gray), and A2 (orange) viscotoxin structures: (a) side chains of 19, 21, 24, 25, and 28 residues are shown and (b) basic amino acid side chains are shown as CPK.

is represented by R25 in viscotoxin C1, which points to the opposite side of the plane. Some have recently suggested that the orientation of the R25 side chain, protruding outside the plane formed by the two α-helices of viscotoxin B, probably acts as an arm that keeps the toxin far from the lipidic interface, thus preventing its insertion into the membrane bilayer (*11*), in agreement with our observation on the requirement of a noncharged residue at this position.

To further correlate the observed mutations with biological activity, the following considerations may be added. It has been recently suggested (*34*), on the basis of fluorescence polarization measurements, that the most active viscotoxin A3 isoform has a high affinity for the most acidic phosphatidylserine (PS) membranes and binds parallel to the surface of the membrane in a so-called carpet-like fashion, perturbing the PS structure through a stiffening effect (*35*). It is worth mentioning that several types of cancer cells, as well as cells undergoing apoptosis, generally have a significant proportion of PS headgroups on the outer leaflet of their membranes. This is a rare occurrence in healthy eukaryotic cells, where lipid asymmetry is actively maintained, and amino phospholipids, such as PS, occur only on the inner leaflet of the membrane (*36*). PS headgroups bear a net negative charge, thus offering a partial explanation for the

observation that cationic antimicrobial peptides, such as viscotoxins, also have antitumoral properties.

The results reported here provide an overall coherent framework for clarifying the mechanism of the action of viscotoxins and open the way to a rational site-directed mutagenesis approach.

ACKNOWLEDGMENT

We gratefully acknowledge the technical support offered by the Large Scale Facilities of Florence (CERM) and the Frankfurt Biophysik Centre.

REFERENCES

1. Orrù, S., Scaloni, A., Giannattasio, M., Urech, K., Pucci, P., and Schaller, G. (1997) Amino acid sequence, S−S bridge arrangement and distribution in plant tissues of thionins from *Viscum album*, *Biol. Chem. 378*, 986−996.
2. Samuelsson, G., and Jayawardene, A. L. (1974) Isolation and characterisation of viscotoxin 1-PS from *Viscum album*, *Acta Pharm. Suec. 11*, 175−184.
3. Bohlmann, H., and Apel, K. (1991) Thionins, *Annu. Rev. Plant Mol. Biol. 42*, 227−240.
4. Bohlmann, H., Clausen, S., Behnke, S., Giese, H., Hiller, C., Ulrich, R. P., Shrader, G., Vibeke, B., and Apel, K. (1988) Leaf-specific thionins of barley: a novel class of cell wall proteins toxic to plant pathogenic fungi and possibly involved in the defense mechanism of plants, *EMBO J. 7*(6), 1559−1565.
5. Huges, P., Dennis, E., Whitecross, M., Llewellyn, D., and Gage, P. (2000) The cytotoxic plant protein, β-purothionin, forms ion channels in lipid membranes, *J. Biol. Chem. 275*, 823−827.
6. Thevissen, K., Ghazi, A., De Samblanx, G. W., Brownlee, C., Osborn, R. W., and Broekaert, W. F. (1996) Fungal membrane responses induced by plant defensins and thionins, *J. Biol. Chem. 271*, 15018−15025.
7. Romagnoli, S., Ugolini, R., Fogolari, F., Schaller, G., Urech, K., Giannattasio, M., Ragona, L., and Molinari, H. (2000) NMR structural determination of viscotoxin A3 from *Viscum album L.*, *Biochem. J. 350*, 569−577.
8. Schaller, G., Urech, K., and Giannattasio, M. (1996) Cytotoxicity of different viscotoxins and extracts from the European subspecies of *Viscum album L.*, *Phytother. Res. 10*, 473−477.
9. Urech, K., Schaller, G., Ziska, P., and Giannattasio, M. (1995) Comparative study on the cytotoxic effect of viscotoxin and mistletoe lectin on tumor cells in culture, *Phytother. Res. 9*, 49−55.
10. Konopa, J., Woynarowski, J. M., and Lewandowska-Gumieniak, M. (1980) Isolation of viscotoxins, cytotoxic basic polypeptides from *Viscum album L.*, *Hoppe-Seyler's Z. Physiol. Chem. 361*, 1525−1533.
11. Coulon, A., Mosbah, A., Lopez, A., Sautereau, A., Schaller, G., Urech, K., Rougè, P., and Darbon, H. (2003) Comparative membrane interaction study of Viscotoxins A3, A2, and B from mistletoe (*Viscum album*) and connections with their structures, *Biochem. J. 374*, 71−78.
12. Piantini, U., Sorensen, O. W., and Ernst, R. R. (1982) Multiple quantum filters for elucidating NMR coupling networks, *J. Am. Chem. Soc. 104*, 6800−6801.
13. Bax, A., and Davis, D. G. (1985) MLEV-17-based two-dimensional homonuclear magnetization transfer spectroscopy, *J. Magn. Reson. 65*, 355−360.
14. Sklenar, V., Piotto, M., Leppik, R., and Saudek, V. (1993) Gradient tailored water suppression for ^{1}H-^{15}N HSQC experiments optimized to retain full sensitivity, *J. Magn. Reson., Ser. A 102*, 241−245.
15. Hwang, T. L., and Shaka, A. J. (1995) Water suppression that works. Excitation sculpting using arbitrary waveforms and pulsed field gradients, *J. Magn. Reson., Ser. A 112*, 275−279.
16. Bartels, C., Xia, T., Billeter, M., Güntert, P., and Wüthrich, K. (1995) The program XEASY for computer-supported NMR spectra analysis of biological macromolecules, *J. Biomol. NMR 5*, 1−10.
17. Wishart, D. S., Bigam, C. G., Holm, A., Hodges, R. S., and Sykes, B. D. (1995) ^{1}H, ^{13}C, and ^{15}N Random Coil Chemical Shifts of the Common Amino Acids: I. Investigations of Nearest Neighbor Effects, *J. Biomol. NMR 5*, 67−81.
18. Wüthrich, K. (1986) Three-dimensional protein structure by NMR, in *NMR of proteins and nucleic acids*, pp 176−199, John Wiley & Sons, Inc., New York.
19. Güntert, P., Mumenthaler, C., and Wüthrich, K. (1997) Torsion angle dynamics for NMR structure calculations with the new program DYANA, *J. Mol. Biol. 273*, 283−298.
20. Güntert, P. (1998) Structure calculation of biological macromolecules from NMR data, *Q. Rev. Biophys. 31*, 145−237.
21. Guex, N., and Peitsch, M. C. (1997) SWISS-MODEL and the Swiss-Pdb Viewer: An environment for comparative protein modeling, *Electrophoresis 18*, 2714−2723.
22. Combet, C., Jambon, M., Deléage, G., and Geourjon, C. (2002) Geno3D: Automatic comparative molecular modeling of protein, *Bioinformatics 18*, 213−214.
23. Fogolari, F., Brigo, A., and Molinari, H. (2002) The Piosson−Boltzmann equation for biomolecular electrostatics: a tool for structural biology, *J. Mol. Recog. 15*, 377−392.
24. Madura, J. D., Briggs, J. M., Wade, R. C., Davis, M. E., Luty, B. A., Llin, A., Antosiewicz, J., Gilson, M. K., Bagheri, B., Scott, L. R., and McCammon, J. A. (1995) Electrostatic and diffusion of molecules in solution: simulations with the University of Houston Dynamics program, *Comput. Phys. Comm. 91*, 57−95.
25. MacKerell, A. D., Jr., Bashford, D., Bellot, M., Dunbrak, R. L., Jr., Field, M. J., Fisher, S., Gao, J., Guo, H., Ha, S., and Joseph, D. et al. (1992) Self-consistent parametrization of biomolecules for molecular modeling and condensed phase simulations, *FASEB J. 6*, A143.
26. Nicholis, A. (1993) *GRASP: Graphical representation and analysis of surface properties*, Columbia University, New York.
27. Brünger, A. T., Clore, G. M., Gronenborn, A. M., and Karplus, M. et al. (1986) Three-dimensional structure of proteins determined by molecular dynamics with interproton distance restraints: application to crambin, *Proc. Natl. Acad. Sci. U.S.A. 83*, 3801−3805.
28. Clore, G. M., Sukumaran, D. K., Gronenborn, A. M., Teeter, M. M., Whitlow, M., and Jones, B. L. (1987) Nuclear magnetic resonance study of the solution structure of α-purothionin. Sequential assignment, secondary structure, and low resolution tertiary structure, *J. Mol. Biol. 193*, 571−578.
29. Lecomte, J. T. J., Jones, B. L., and Llinas, M. (1982) Proton magnetic resonance studies of barley and wheat thionins: structural homology with crambin, *Biochemistry 21*, 4843−4849.
30. Lecomte, J. T. J., Kaplan, D., Thunberg, E., and Samuelsson, G. (1987) Proton magnetic resonance characterization of phoratoxins and homologous proteins related to crambin, *Biochemistry 26*, 1187−1194.
31. Lankisch, P. G., and Vogt, W. (1971) Potentiation of hemolysis by the combined action of phospholipase A and a basic polypeptide containing an S−S bond, *Experientia 2*, 122−123.
32. Corzo, G., Escoubas, P., Villegas, E., Barnham, K. J., He, W., and Norton, R. (2001) Characterization of unique amphipathic antimicrobial peptides from venom of the scorpion *Pandinus imperator*, *Biochem. J. 359*, 35−45.
33. Richard, J. A., Kelly, I., Marion, D., Pezolet, M., and Auger, M. (2002) Interaction between β-Purothionin and Dimyristoylphosphatidylglycerol: a ^{31}P NMR and Infrared Spectroscopic Study, *Biophys. J. 83*, 2074−2083.
34. Coulon, A., Berkane, E., Sautereau, A. M., Urech, K., Rougé, P., and Lopez, A. (2002) Modes of membrane interaction of a natural cysteine-rich peptide: viscotoxin A3, *Biochim. Biophys. Acta 1559*(2), 145−159.
35. Shai, Y. (1999) Mechanism of the binding, insertion, and destabilization of phospholipid bilayer membranes by α-helical antimicrobial and cell nonselective membrane-lytic peptides, *Biochim. Biophys. Acta 1462*, 55−70.
36. Vogel, H. J., Schibli, D. J., Jing, W., Lohmeier-Vogel, E. M., Epand, R. F., and Epand, R. M. (2002) Toward a structure−function analysis of bovine lactoferricin and related tryptophan- and arginine-containing peptides, *Biochem. Cell Biol. 80*, 49−63.

BI034762T